

Article

Weight Loss, Thermodynamics, SEM, and Electrochemical Studies on N-2-Methylbenzylidene-4-antipyrineamine as an Inhibitor for Mild Steel Corrosion in Hydrochloric Acid

Israa Abd Alkadir Aziz ¹, Makarim H. Abdulkareem ¹ , Iman Adnan Annon ¹, Mahdi M. Hanoon ¹, Mohammed H. H. Al-Kaabi ², Lina M. Shaker ^{3,4}, Ahmed A. Alamiery ^{4,5,*} , Wan Nor Roslam Wan Isahak ⁴  and Mohd S. Takriff ^{4,6}

¹ Production Engineering and Metallurgy, University of Technology, Baghdad 10001, Iraq; iraa.a.aziz@uotechnology.edu.iq (I.A.A.A.); 70008@uotechnology.edu.iq (M.H.A.); 70039@uotechnology.edu.iq (I.A.A.); 70182@uotechnology.edu.iq (M.M.H.)

² College of Industrial Management of Oil and Gas, Basrah University of Oil and Gas, Basrah 61001, Iraq; drmh1962@gmail.com

³ Medical Instruments Technology Engineering, Al Mansour University College, Baghdad 10001, Iraq; p109960@siswa.ukm.edu.my

⁴ Department of Chemical and Process Engineering, Faculty of Engineering and Built Environment, University Kebangsaan Malaysia (UKM), P.O. Box 43000, Bangi 43600, Malaysia; wannorrosalam@ukm.edu.my (W.N.R.W.I.); sobritakriff@ukm.edu.my (M.S.T.)

⁵ Energy and Renewable Energies Technology Center, University of Technology, Baghdad 10001, Iraq

⁶ Chemical and Water Desalination Engineering Program, Department of Mechanical & Nuclear Engineering, College of Engineering, University of Sharjah, Sharjah P.O. Box 26666, United Arab Emirates

* Correspondence: dr.ahmed1975@ukm.edu.my or dr.ahmed1975@gmail.com



Citation: Aziz, I.A.A.; Abdulkareem, M.H.; Annon, I.A.; Hanoon, M.M.; Al-Kaabi, M.H.H.; Shaker, L.M.; Alamiery, A.A.; Isahak, W.N.R.W.; Takriff, M.S. Weight Loss, Thermodynamics, SEM, and Electrochemical Studies on N-2-Methylbenzylidene-4-antipyrineamine as an Inhibitor for Mild Steel Corrosion in Hydrochloric Acid. *Lubricants* **2022**, *10*, 23. <https://doi.org/10.3390/lubricants10020023>

Received: 7 December 2021

Accepted: 29 January 2022

Published: 9 February 2022

Publisher's Note: MDPI stays neutral with regard to jurisdictional claims in published maps and institutional affiliations.



Copyright: © 2022 by the authors. Licensee MDPI, Basel, Switzerland. This article is an open access article distributed under the terms and conditions of the Creative Commons Attribution (CC BY) license (<https://creativecommons.org/licenses/by/4.0/>).

Abstract: The use of N-2-methylbenzylidene-4-antipyrineamine as an acid corrosion inhibitor for mild steel surfaces in hydrochloric acid is discussed in this article by means of weight loss, electrochemical impedance spectroscopy (EIS), and scanning electron microscopy (SEM) methods. The experimental findings exhibited that N-2-methylbenzylidene-4-antipyrineamine is a significant corrosion inhibitor for the mild steel in 1.0 M HCl solution and that its protection efficiency touches the peak at 5×10^{-4} M, exhibiting 91.8% for N-2-methylbenzylidene-4-antipyrineamine. The inhibitory efficiency increases as the inhibitor concentration rises and reduces as the temperature rises. Temperature has a significant impact on corrosion and blocking activities, which is extensively examined and explained. According to the gravimetric results, the examined inhibitor inhibits mild steel surface corrosion by providing a barrier at the metal–hydrochloric acid medium interface. Thermodynamic characteristics were combined with a quantum chemistry investigation using density functional theory to provide more insight into the inhibitory effect mechanism. The tested inhibitor adsorbs on the mild steel surface based on Langmuir's adsorption isotherm method.

Keywords: corrosion inhibitor; antipyrineamine; methylbenzylidene; gravimetric; EIS

1. Introduction

Mild steel is easily corroded in everyday situations. Acid solutions, particularly hydrochloric acid, are typically very aggressive media for mild steel corrosion. They are employed in various industrial operations such as acid cleaning, oil-well acidizing, acid descaling, and so on [1–3]. Because of its outstanding mechanical qualities and inexpensive cost, mild steel is frequently used as a structural material in various chemical and petrochemical industries [4]. Mild steel's major point is that it dissolves in acidic conditions. Inhibitors are among the most practical ways to prevent mild metal from corrosion, particularly in acid conditions. At quite low doses, the inhibitors are efficient. The use of inhibitors has resulted in a decreased rate of iron dissolution and a significant increase

in the life of mild steel [5]. Organic molecules containing nitrogen, sulfur, and oxygen atoms are the most well-known acidic inhibitors. Organic molecules are thought to prevent corrosion by adsorbing onto metal surfaces. Moreover, the electronic structure of inhibiting molecules, steric factor, aromaticity, and electron density at the donor site, the existence of functional groups which include $-C=N-$, $-C=O$, $-N=N-$, etc., molecular area, the molecular weight of the molecule, temperature, and electrochemical potential at the metal/solution interface are all factors that influence adsorption [6]. Inorganic compounds or their mixtures, including such phosphates, chromate, nitrite, and the salts of zinc, silicates, cadmium, and arsenic have already been proved to be efficient as corrosion inhibitors for the mild steel in the metal industries for a long time [7]. However, their own toxic effects are a significant disadvantage, and their use may cause reversible (temporary) or irreversible (permanent) damage to organ systems. As a result, the development of more eco-friendly corrosion inhibitors is of tremendous practical importance. Due to the chemical structure of N-2-methylbenzylidene-4-antipyrineamine which contains nitrogen, oxygen, and sulfur heteroatoms as well as benzene rings, it can transfer its electrons into unoccupied d-orbitals of iron atoms on the surface of mild steel to produce a strong metal-protective coating by coordinate bonding [8–15]. As a result, N-2-methylbenzylidene-4-antipyrineamine has the potential to be a corrosion inhibitor in hydrochloric acid environments [16–20]. We wish to look into the impact of immersion time and solution temperature on corrosion inhibition mechanisms in this study. The EIS and weight loss techniques was used to test the N-2-methylbenzylidene-4-antipyrineamine inhibitive ability on mild steel corrosion in 1 M HCl. SEM surface morphology tests were performed to ensure that the researched N-2-methylbenzylidene-4-antipyrineamine protects the steel surface from corrosion in the tested media. Herein, we describe the evaluation of N-2-methylbenzylidene-4-antipyrineamine (Figure 1) as a metallic corrosion inhibitor in a corrosive solution using gravimetric and EIS methods. The exposure periods were also investigated. The process of inhibition was also subjected to a suitable adsorption isotherm.

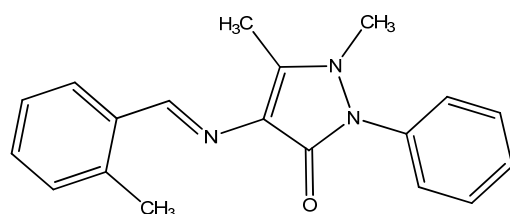
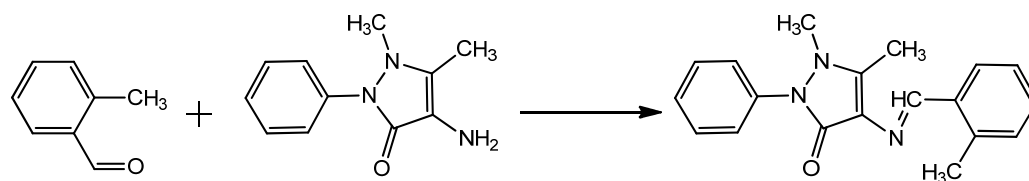


Figure 1. Structure of N-2-methylbenzylidene-4-antipyrineamine.

2. Materials and Methods

2.1. Inhibitor

A solution of 2-methylbenzaldehyde (0.1 mmol) in 50 mL ethanol was refluxed with 4-amino-1,5-dimethyl-2-phenyl-1H-pyrazol-3(2H)-one (0.1 mmol) for 5 h. After cooling to room temperature, a solid mass was separated and recrystallized from ethanol in 87% yield: $^1\text{H-NMR}$ (CDCl_3): δ 9.712 (s, $\text{N}=\text{C}-\text{H}$), 6.983, 7.214, 7.307, 7.322, 7.418, 7.675, 7.711, 7.775, 7.876 (s, 1H, aromatic ring), δ 2.017 (s, 3H, CH_3), 2.964 (s, 3H, CH_3), δ 3.128 (s, 3H, CH_3); IR: 3050.0, 3061.6 cm^{-1} (C–H, aromatic), 2910.7, 2945.9, and 2970.0 cm^{-1} (C–H, aliphatic), 1646.6 cm^{-1} (C=O), 1569.4 cm^{-1} (C=C); 1588.6 cm^{-1} (C=N, imine), 1484.4 cm^{-1} (C=C, aromatic); UV-Vis: 250 nm in acetonitrile. The reaction sequence was postulated in Scheme 1.



Scheme 1. The chemical synthesis of target inhibitor.

2.2. Materials

Mild steel coupons purchased from the Company of Metal Samples have been utilized during the current investigation as the working electrodes. The mild steel chemical composition weight percentage is presented in Table 1. The mild steel coupons were cleaned based on the standard method G1-03/ASTM [21].

Table 1. Chemical composition of the mild steel coupon (wt.%).

Carbon	Manganese	Silicon	Aluminum	Sulfur	Phosphorus	Iron
0.210	0.050	0.380	0.010	0.050	0.090	balance

2.3. Electrochemical Impedance Spectroscopy

The tests were carried out in aerated, non-stirred 1.0 M HCl solutions containing various doses of the inhibitor. A Gamry water-jacketed glass cell was used to conduct electrochemical studies at the steady-state corrosion potential. The cell had three electrodes: a working electrode, a counter electrode, and a reference electrode made of a steel specimen, a graphite bar, and a saturated calomel electrode (SCE). The Gamry Instrument Potentiostat/Galvanostat/ZRA (REF 600) model was used for the experiments (Gamry, Warminster, PA, USA). The corrosion potential of the electrochemical impedance spectroscopy was measured using Gamry's DC105 and EIS300 software (EIS). The AC signals of 5 mV peak-to-peak amplitude at the corrosion potential in the frequency range of 100 KHz to 0.1 Hz were used for EIS experiments. Using the Gamry Echem Analyst programme, all impedance data were fitted to appropriate equivalent circuits (ECs). To enable the steady-state potential to establish, the electrochemical tests started about 30 min after the working electrode was immersed in the solution. To ensure that the tests were repeatable, each measurement was carried out in triplicate and only the average data were presented [22].

2.4. Weight Loss Measurements

Weight loss techniques were conducted at periods of time of (1, 6, 12, and 24 h) at temperatures (30, 40, 50, and 60 °C) utilizing an electrical balance. Weight loss measurements were conducted at the inhibitor concentrations of 1×10^{-4} , 2×10^{-4} , 3×10^{-4} , and 5×10^{-4} M and after exposure time, the mild steel was removed, carefully washed with distilled water, acetone, dried in the oven, and weighted. The measurements were carried out in triplicate and the weight loss mean value was evaluated [23].

2.5. Acidic Solution

The corrosive solution was prepared by diluting 37% HCl (Merck-Malaysia) using distilled water.

3. Results and Discussion

3.1. EIS

The EIS findings for the mild steel corrosion in the absence and presence of the N-2-methylbenzylidene-4-antipyrineamine are presented in Table 2. The impedance spectra for the different concentrations of N-2-methylbenzylidene-4-antipyrineamine at 30 °C are displayed in Figure 2. As exhibited in Figure 1, a significant improvement in the total substrate impedance was recognized with the addition of the N-2-methylbenzylidene-4-antipyrineamine concentration hydrochloric acid environment. The mild steel impedance

spectra in the presence of N-2-methylbenzylidene-4-antipyrineamine with the Nyquist plots had two loops: the first one in the HF field (high frequency) and the second one at an MF region (intermediate frequency), with a slight inductive performance at LF (low frequency). The electrode and the charge-transfer process were responsible for the HF and MF loops, respectively. In the absence or presence of N-2-methylbenzylidene-4-antipyrineamine, the inductive behavior seen in the LF zone was related to either the relaxation of the adsorption of corrosion results or the adsorption of N-2-methylbenzylidene-4-antipyrineamine molecules on the surface of mild steel in the corrosive environment [24]. The protection efficiency was determined from the charge-transfer resistance according to Equation (1):

$$IE(\%) = \frac{R_{ct}^- - R_{ct}}{R_{ct}^-} \times 100 \quad (1)$$

where R_{ct}^- represents the charge-transfer resistance value with the addition of the tested inhibitor whereas R_{ct} indicates the charge-transfer resistance value in the absence of the corrosion inhibitor. As seen from Table 2, the protection efficiency increases with increasing the inhibitor concentration. The parallel network $R_{ct} - C_{dl}$ (charge-transfer resistance double-layer capacitance) is frequently a poor approximation in these instances, particularly in techniques with an effective corrosion inhibitor. Because the mild steel corroding surface is assumed to be inhomogeneous in a corrosive environment due to its roughness, the capacitance is reported using a CPE (constant phase element).

Table 2. The parameters of EIS for mild steel in 1.0 M HCl with different inhibitor concentrations at 30 °C.

Inhi. Conc., (M)	R_s , ohm cm^2	R_{ct} , ohm cm^2	$\text{CPE}_{dl} (Y_0 \times 10^{-5})$, ohm $^{-1}$ cm^{-2} S^n	IE (%)
Blank	–	77.0	–	0.0
1×10^{-4}	1.550	239.0	39.40	71.08
2×10^{-4}	1.560	259.0	22.20	75.0
3×10^{-4}	1.630	328.0	17.70	77.0
5×10^{-4}	1.730	376.0	23.30	80.0

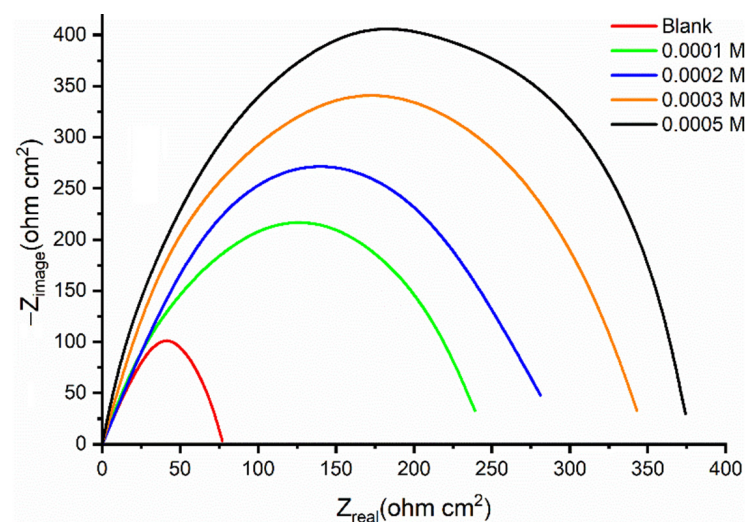


Figure 2. Mild steel Nyquist plots in 1.0 M HCl with different inhibitor concentrations.

3.2. Weight Loss Measurements

The corrosion rate and protection efficiency of the inhibitor at various concentrations (1×10^{-4} , 2×10^{-4} , 3×10^{-4} , and 5×10^{-4} M) and different temperatures (30–60 °C) were evaluated by gravimetric techniques, and the results are demonstrated in Figures 3 and 4. The protection efficiency increased by increasing the inhibitor concentration, and a decrease in the corrosion rate was shown at all studied concentrations, as illustrated in Figure 3. Hence, it is obvious that the protection efficiency was concentration-dependent. With increasing inhibitor concentration, considerable inhibitor molecules' numbers are adsorbed on the tested coupon surface, which appears in increased protection performance. The adsorbed inhibitor molecules control and/or block the reaction sites and hence protect the coupon surface from the corrosive solution. While the inhibitor has significant ion pairs of electrons, such as ion pairs on sulphur, and nitrogen atoms, and the pi-electrons, that are coordinately bonded with iron atoms on the coupon surface, they could retard corrosion. For the inhibitor concentration of 5×10^{-4} M and 30 °C, and an immersion time of 5 h, the inhibitor exhibited the highest protection efficiency of 91.8%. The experimental findings as in Figure 3 revealed that the mass loss and the rate of corrosion increased with the exposure period for the tested coupons and at all the studied concentrations of the tested inhibitor [25]. At 24 h of exposure period in the presence of the tested inhibitor, the corrosion rate increased slightly. Thus, the slight increase in corrosion could be attributed to the increased immersion time in the acidic solution. Figure 3 shows a plot of the corrosion rate with inhibition efficiency (%) versus time (hours) for various inhibitor concentrations. From these results, it can be seen that the inhibition efficiency increased with increasing time significantly for all levels of inhibitor concentration. Then, a decrease in the value was observed after 24 h and depending on the concentration of the inhibitor. The corrosion rate and protection efficiency were determined according to Equations (2) and (3):

$$C_R = \frac{87600W}{atd} \quad (2)$$

where W represents the coupon weight loss in "g", a refers to the coupon surface area in cm^2 , t signifies to the immersion period in h, and d is the coupon density in g/cm^3 .

$$IE\% = \left[\frac{C_{R(o)} - C_{R(i)}}{C_{R(o)}} \times 100 \right] \quad (3)$$

where $C_{R(o)}$ and $C_{R(i)}$ are the corrosion rate in the absence and presence of the inhibitor, respectively.

The current inhibitor's (N-2-methylbenzylidene-4-antipyrineamine) inhibitory efficiency in hydrochloric acid solution can also be evaluated with that of other published inhibitors that are using corrosion inhibitors generated from antipyrine to protect mild steel from corrosion. The majority of antipyrine studied exhibit substantial inhibitory effectiveness, as seen in Table 3. To draw a parallel with the current inhibitor, N-2-methylbenzylidene-4-antipyrineamine has the highest inhibition performance of the antipyrine listed in Table 3 [26–31], and a performance comparable to that stated in [28,30]. The corrosion rate was lowered and the corrosion inhibition performance increased as the concentration of N-2-methylbenzylidene-4-antipyrineamine increased. This may be due to the fact that as the N-2-methylbenzylidene-4-antipyrineamine concentration rises, the inhibitor's adsorption coverage on steel surfaces increases.

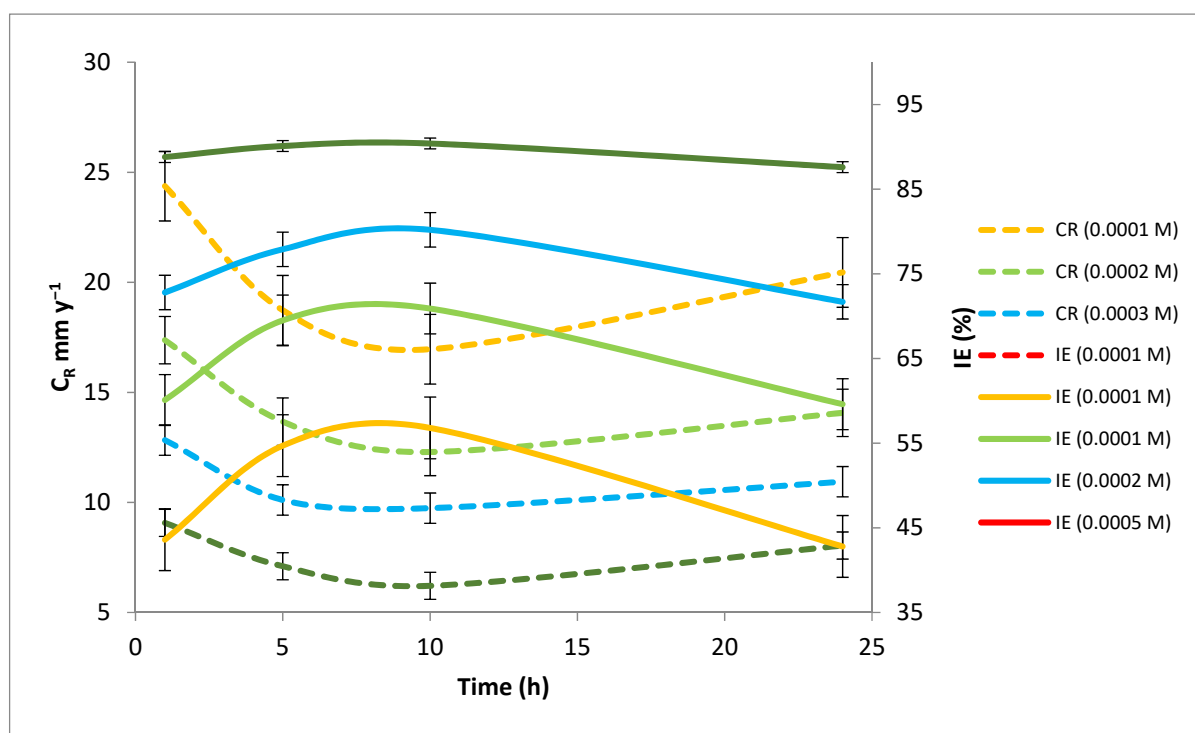


Figure 3. Mild steel corrosion plot in 1.0 M HCl with different inhibitor concentrations at various immersion times.

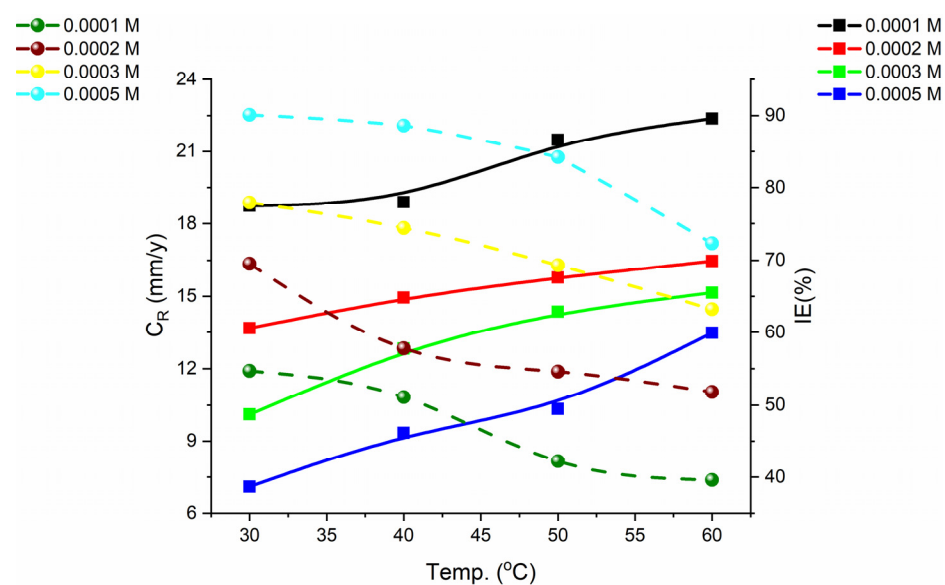


Figure 4. Mild steel corrosion plot in 1.0 M HCl with different inhibitor concentrations at various temperatures.

Table 3. The performance of N-2-methylbenzylidene-4-antipyrineamine inhibition was evaluated numerically to that of other antipyrine that had previously been studied.

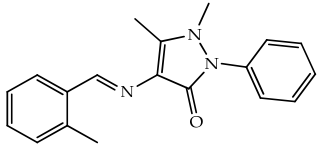
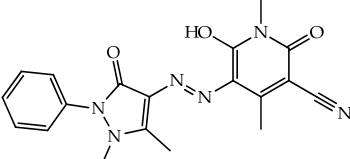
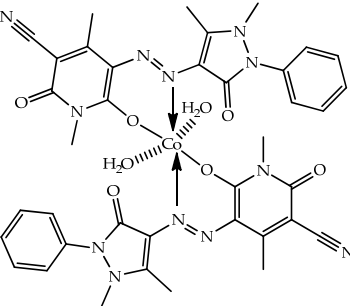
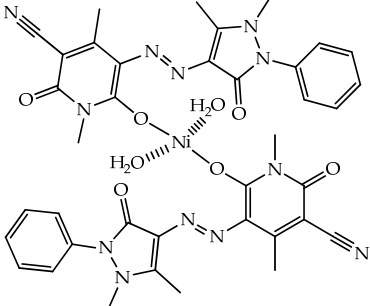
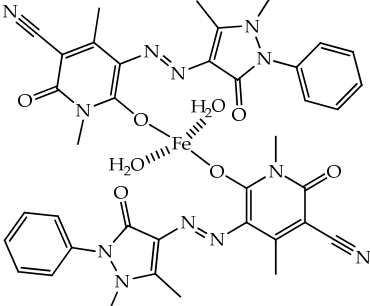
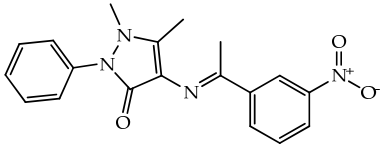
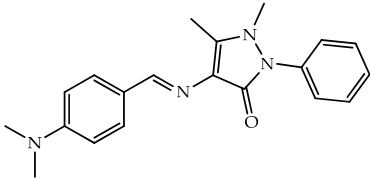
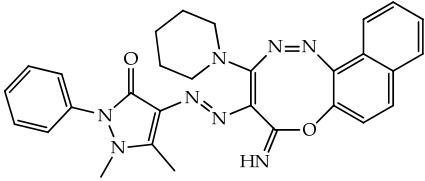
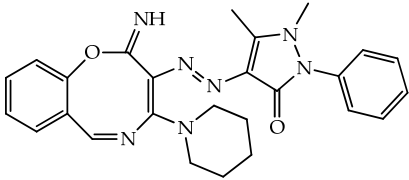
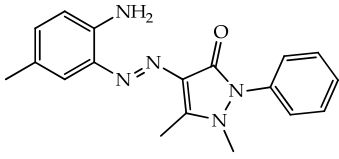
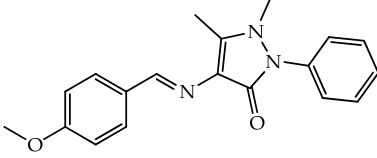
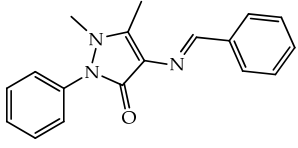
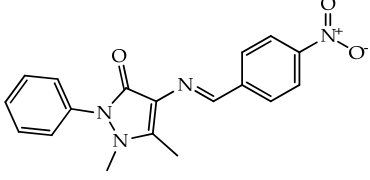
Inhibitor	Inhibitor Concentration	IE%	Refs.
	0.0005 M	91.8	Current inhibitor
	25 mg/L	75	[26]
	25 mg/L	81.25	[26]
	25 mg/L	89.33	[26]
	25 mg/L	79.43	[26]
	4 mM	87	[27]

Table 3. Cont.

Inhibitor	Inhibitor Concentration	IE%	Refs.
	0.5 mM	95	[28]
	8.0 μ M	87.5	[29]
	8.0 μ M	86.1	[29]
	0.01 M	95	[30]
	11×10^{-6} M	47.9	[31]
	11×10^{-6} M	45.5	[31]
	11×10^{-6} M	41.7	[31]

The increase in surface coverage due to the adsorption of inhibitor molecules on the mild steel surface is ascribed to the improvement in protective efficacy. The adsorption layer then protects the mild steel surface from the acidic environment by blocking the active sites. In comparison to the first examined antipyrine inhibitors in Table 3, N-2-methylbenzylidene-4-antipyrineamine demonstrated superior protection against corrosion. The impacts of steric hindrance and heteroatoms in the inhibitor molecular structure are linked to this phenomenon. The best inhibiting efficiency was found when the inhibitor was added to the corroding solution at a concentration of 0.0005 M. The inhibiting performance did not alter much when the concentration was increased to 0.001 M. After 5 h of immersion, the greatest corrosion inhibition efficiency of around 91 percent was observed at 0.0005 M concentration. After 5 h of exposure time, there was no considerable rise in corrosion inhibition efficiency,

and after 24 h, inhibition efficiency declined. This was due to the desorption of the examined inhibitor molecules from the mild steel surface and the destabilization of the protective barrier on the mild steel surface [32]. After 24 h of immersion, there was a significant decrease in inhibitory performance.

Temperature highly affects the corrosion rate and the inhibition efficiency, and with increasing temperature, the rate of corrosion increases exponentially in an acidic environment. To understand the protection performance of the tested inhibitor at various temperature degrees, 30–60 °C, the corrosion rate and inhibition efficiency were investigated (Figure 4). The tested inhibitor revealed the highest inhibition efficiency at 30 °C, which regularly declined with an increase in temperature. The tested inhibitor exhibited lower protection performance at the maximum temperature. This result attends to the fact that the rise in temperature did not support physisorption (physical interactions), therefore reducing the protection performance.

The corrosion process activation parameters were determined according to Arrhenius Equation (4):

$$\log C_R = \log k - \left\{ \frac{E_a}{2.303RT} \right\} \quad (4)$$

where E_a is the activation energy, k represents the frequency factor, T is the temperature, and R refers to the gas constant.

The value of the metal coupon in 1 M hydrochloric acid solution without and with various concentrations of the examined inhibitor have been evaluated based on the plot between $\log C_R$ and $1/T$ as seen in Figure 5 [33]. The E_a was computed and given in Table 4 using a linear graph with a slope of $-E_a/2.303R$ as shown in Figure 5. As the temperature rose, the adsorption of inhibitor molecules on the metal surface decreased, and the corrosion rate rose in response. The adsorption of inhibitor molecules on the mild steel surface diminished as the temperature rose, and the rate of corrosion rose in response.

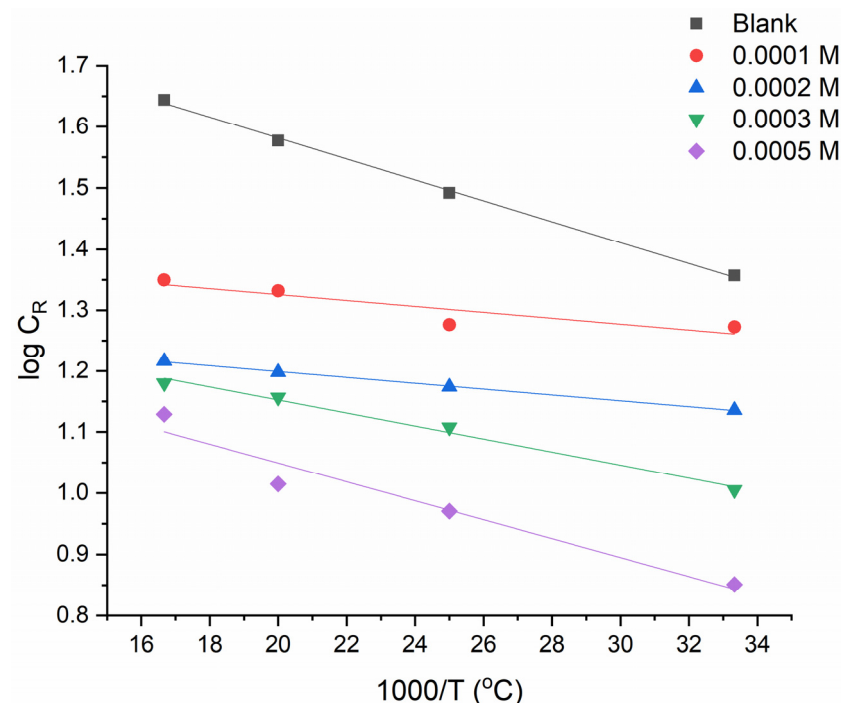


Figure 5. The $\log C_R$ vs. $\frac{1}{T}$ plot for the different concentrations of N-2-methylbenzylidene-4-antipyrineamine and various temperatures.

Table 4. The values of isothermic parameters for mild steel in 1 M HCl without and with the addition of various concentrations of the tested inhibitor.

C (M)	E_a (kJ·mol ^{−1})	ΔH_a (kJ·mol ^{−1})	ΔS_a (J·mol ^{−1} K ^{−1})
Blank	63.11	60.43	57.58
0.0001	49.37	45.77	131.74
0.0002	46.28	43.17	119.32
0.0003	45.21	42.48	114.73
0.0005	43.84	41.32	109.99

The fact that the inhibitory processes have a greater activation energy than the uninhibited indicates that the dissolution of mild steel occurs gradually. Moreover, as the concentration of the inhibitor rose, the activation energies rose with it. This indicates that the presence of the inhibitor creates a barrier to the corrosion reaction, which increases with increasing concentration. At higher temperatures, the adsorption of the inhibitor molecules on the metal surface decreases, and as a result, corrosion rates increase.

Based on Equation (5), a modified Arrhenius plot of $\log C_R/T$ against $1/T$ for mild steel dissolution in 1 M HCl enabled the determination the activation enthalpy (ΔH_a) and the activation entropy (ΔS_a) values:

$$\log \left\{ \frac{C_R}{T} \right\} = \left[\left\{ \log \left\{ \frac{R}{Nh} \right\} + \left\{ \frac{\Delta S_a}{2.303R} \right\} \right\} \right] - \left(\frac{\Delta H_a}{2.303RT} \right) \quad (5)$$

where N is the number of Avogadro and h is the of Plank constant.

Figure 6 shows a plot of $\log(C_R/t)$ vs. $1/t$. Table 4 shows the activation enthalpy (ΔH_a) and the activation entropy (ΔS_a) values calculated from the slope and intercept of Figure 6. The positive ΔH_a (63 – 43 kJ·mol^{−1}) values illustrate the endothermic nature of mild steel dissolving. The kinetic characteristics of activation are mostly responsible for the low corrosion rate, as seen by the increase in H with increasing inhibitor concentration. The enthalpy of activation values in the absence (0.0 ppm) and in the presence of the tested inhibitor (0.0005 M) were 60 kJ·mol^{−1} and 41 kJ·mol^{−1}, respectively (Table 4), and were obtained from the slope of Figure 6, whereas the entropy of activation values in the absence and in the presence of the tested inhibitor were 57 J·mol^{−1} and 109 J·mol^{−1}, respectively, and were determined from the intercept of Figure 6. Positive ΔH_a values without and with the addition of the tested inhibitor suggest that the mild steel dissolving process is endothermic [34,35].

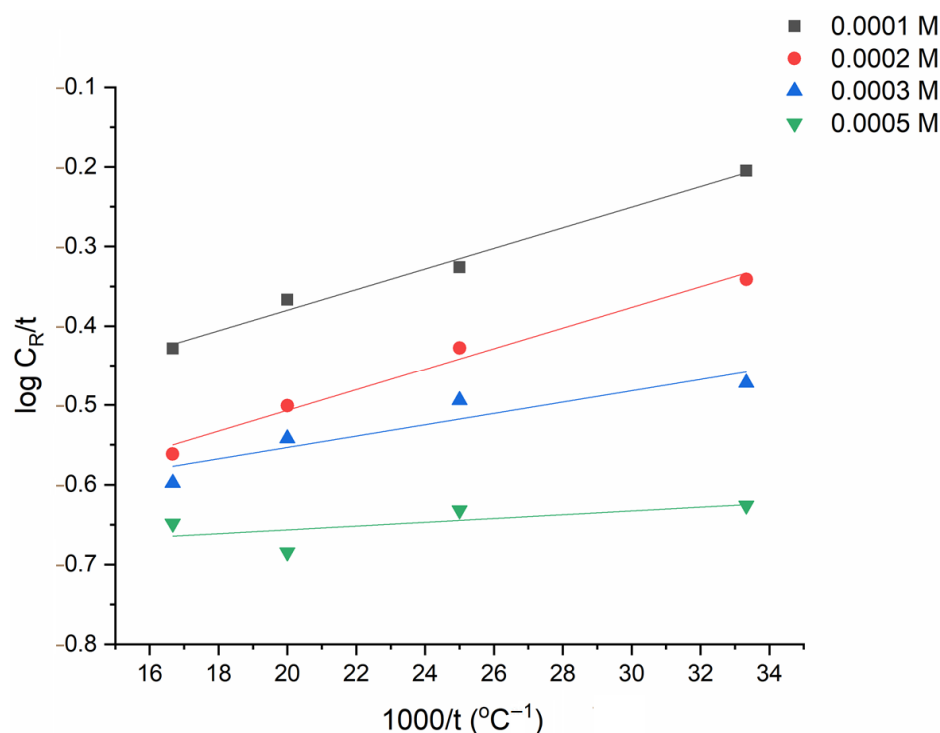


Figure 6. Arrhenius modified plot between $\log C_R/t$ and $1/t$ for mild steel with the addition of various concentrations of the tested inhibitor.

3.3. Adsorption Isotherm

Generally, the ability of the investigated inhibitor molecules to be adsorbed on the metallic surface determines their protective efficacy. As a result, it is critical to comprehend the adsorption isotherm, which offers crucial information on the inhibitor molecules' interactions with the surface of the metal. The nature and chemical structure of the inhibitor molecules, and also how they are adsorbed on the metal surface (physisorption or chemisorption), influence the corrosion inhibitory mechanism of the metallic surface [36–40]. The inhibitory concentrations and surface coverage (θ) were studied using several adsorption techniques to determine the best adsorption behavior. In the 1 M HCl solution, the equilibrium adsorption of the studied inhibitor obeyed the Langmuir adsorption principle on the alloy. Surface coverage was related to inhibitor concentration and equilibrium constant (K_{ads}) in this Langmuir model, as shown in Equation (6)

$$\frac{C}{\theta} = \frac{1}{K_{ads}} + C \quad (6)$$

Figure 7 shows a straight line generated by graphing C/θ versus C , with a linear correlation coefficient (R^2) close to one, indicating that the adsorption process of the examined inhibitor's molecules in the acidic medium on the metallic surface fits the Langmuir concept. The value of ΔG_{ads}^0 was calculated using Equation (7) [41]:

$$\Delta G_{ads}^0 = -2.303 RT \log 55.5 K_{ads} \quad (7)$$

where R is the universal gas constant, T is the absolute temperature, and the 55.5 represents the value of the molar concentration ($\text{mol}\cdot\text{L}^{-1}$) of water. Early investigations have shown that if the value of ΔG_{ads}^0 is negative, the inhibitor molecule's adsorption on the metallic surface is a natural process [42]. In the present study, the value of ΔG_{ads}^0 for the tested inhibitor is $-33.85 \text{ kJ}\cdot\text{mol}^{-1}$, implying that the adsorption process is indeed physisorption and chemisorption [43,44].

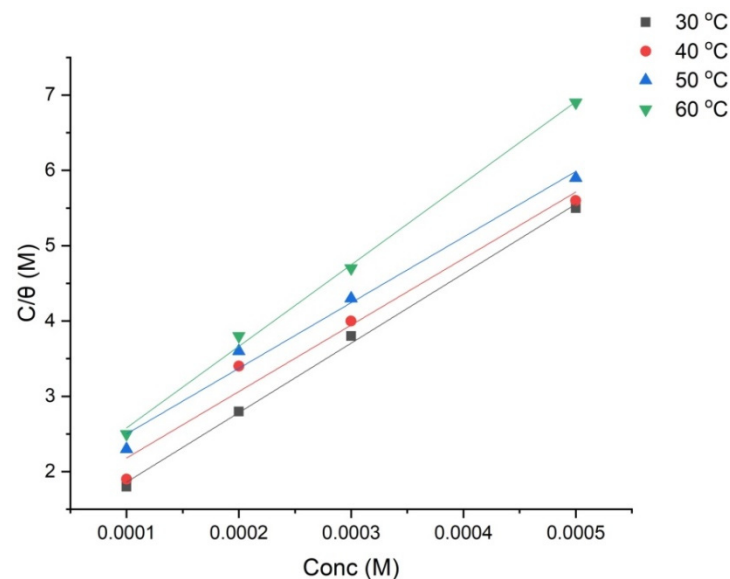


Figure 7. The plot of Langmuir's adsorption isotherm model for the examined inhibitor in 1 M HCl on the metallic surface at the various temperatures.

3.4. Surface Morphology

The surface morphology investigation (SEM) for the mild steel coupons immersed for 5 h in a solution of 1 M hydrochloric acid solution in the absence and presence of the optimum concentration (5×10^{-4} M) of the N-2-methylbenzylidene-4-antipyrineamine has been postulated in Figure 8. From the SEM images as in Figure 8a, it can be seen that the significant damage on the mild steel surface was fulfilled with the corrosion product while, with Figure 8b, after adding the optimum concentration of N-2-methylbenzylidene-4-antipyrineamine, the mild steel surface became more smooth.

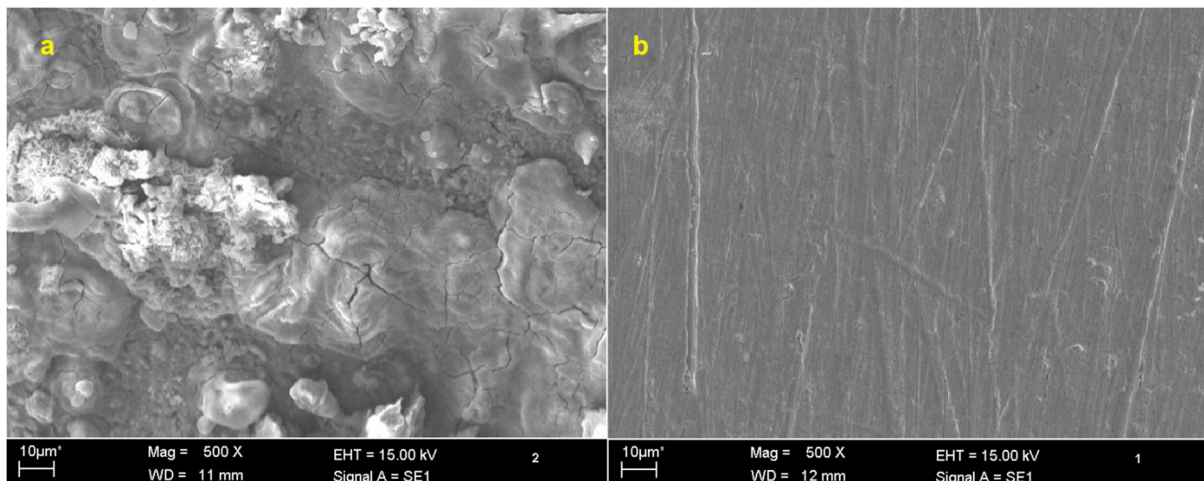


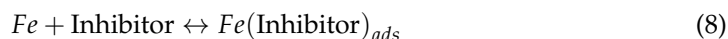
Figure 8. SEM images of mild steel coupons in the absence (a) and presence (b) of the tested inhibitor.

3.5. Possible Mechanisms of Inhibition

Organic inhibitors, in general, work via adsorption to prevent the corrosion of mild steel [45–49]. This includes adsorbed inhibitor molecules replacing adsorbed water molecules and other corrosive substances on the surface of the mild steel [47–49]. The inhibition mechanism is influenced by a number of variables [47–49]. The metallic surface charges and the state of natural and/or synthetic organic molecules in an acidic solution, in particular, have a significant impact on the adsorption mechanism [50]. The surface of mild steel in the hydrochloric acid medium is positively charged, and anions (chloride ions) selectively

adsorbed on the surface, according to previous research investigations [51,52]. Excess electrons on the surface are created by various adsorbents, allowing cationic particles to be adsorbed on the mild steel surface [47–52]. The investigated inhibitor would undoubtedly be protonated in a 1 M hydrochloric acid environment and electrostatically pulled onto the mild steel surface (physical adsorption). The physisorption process includes the following: Cl in HCl was thought to first unite with the surface of the metal (positively charged) via Coulomb force, and then the inhibitor molecule was adsorbed between the positively charged molecular and negatively charged mild steel surface via ionic attraction. These adsorbed molecules formed a monomolecular film when they reacted with $[\text{Fe}(\text{H}_2\text{O})\cdot 2\text{Cl}]$. To achieve stability, cations received electrons from the steel surface. The electron density of N, and O atoms in the inhibitor molecule were enhanced by anions, which are considered donating groups.

On the surface, nitrogen and/or oxygen heteroatoms could be liberated. Through the donor–acceptor contact, the electron pair in the examined inhibitor molecules might establish coordination and back-donating bonds with the iron atoms which have vacant d-orbital in addition to π -electrons (chemical adsorption). Chemisorption is accomplished through a mechanism known as retro-donation. As a result, a coating layer is applied to the mild steel surface to shield it from the acidic media. The role of inhibitors is chemically interpreted by absorbing them on steel surfaces, forming a protective thin layer (blocking cathodic and/or anodic processes) or chemical bonding. This is due to the metal's interaction with the inhibitor molecules. The inhibitory process can be continued using three adsorption mechanisms. The first is charged molecules that attract metals electrostatically. The interaction between the surface and unbound electrons is the second process. The metal surface and π -electron interaction is the final mechanism. Our mild steel corrosion inhibitor may be explained in terms of the number of adsorption sites, charge density, molecule size, inhibitor interaction with metal surface method, and ability to form an insoluble complex in 1 M of HCl. Figure 1 shows the π -electrons implicated in both unpaired electrons and double bonds on nitrogen and oxygen atoms derived from chemical interactions with the metallic surface. Figure 9 illustrates the hypothesized inhibitory mechanism. Figure 9 suggests the mechanism of corrosion inhibition of mild steel in 1 M HCl medium by N-2-methylbenzylidene-4-antipyrineamine molecules. The existence of N-2-methylbenzylidene-4-antipyrineamine layers on the steel surface prevented acidic ions from penetrating the surface and thereby preserved the surface. N-2-methylbenzylidene-4-antipyrineamine should have formed the protective surface coating via nitrogen and oxygen heteroatoms as well as the pi-bonds. The physical adsorption of the examined inhibitor molecules on the mild steel surface was caused by the electrostatically attractions of the protonated N-2-methylbenzylidene-4-antipyrineamine molecules and the preadsorbed counter chloride ions on the mild steel surface. Between these chemical groups and Fe's empty orbital, donor–acceptor interactions could occur. With any antibonding orbitals, back-donation is also a possibility (Equations (8)–(10)).



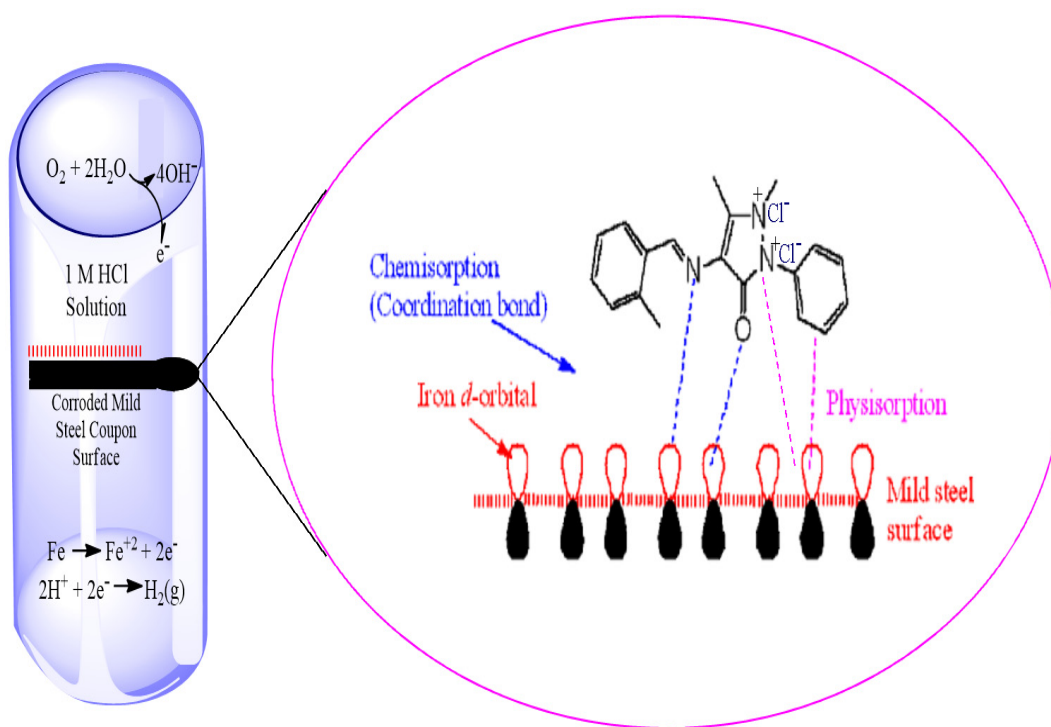


Figure 9. The hypothesized inhibitory mechanism of the examined inhibitor on the mild steel surface in corrosive medium.

4. Conclusions

The study's findings can be summarized as follows:

1. A Schiff base derived from an environmentally beneficial molecule called antipyrine was produced and tested as a mild steel corrosion inhibitor in a 1 M HCl solution at temperatures ranging from 30 to 60 °C.
2. Although the investigated corrosion inhibitor has an inhibitory impact on mild steel in the analyzed corrosive medium, the findings indicate that N-2-methylbenzylidene-4-antipyrineamine is a significantly improved inhibitor. N-2-methylbenzylidene-4-antipyrineamine, derived from the mass loss approach, protected the mild steel surface by 91.8 percent at 30 °C.
3. The inhibitory efficacy of the tested inhibitor is shown to diminish as the temperature rises from 30 to 60 °C. At 60 degrees Celsius, the inhibition efficiency decreases marginally.
4. The synthesized N-2-methylbenzylidene-4-antipyrineamine has significant corrosion inhibition efficiency in the mild steel in 1 M hydrochloric acid environment owing to the presence of the highly efficient electronic sites (sulphur, nitrogen, and pi-bonds) that block the active sites of mild steel.
5. The electrochemical impedance spectroscopy and weight loss techniques exhibited that the protection performance increases with increasing the concentration.
6. The value of ΔG_{ads}^0 is negative, the inhibitor molecule's adsorption on the metallic surface is a natural process.
7. The value of ΔG_{ads}^0 is $-33.85 \text{ KJ} \cdot \text{mol}^{-1}$, suggesting physisorption and chemisorption adsorption mechanisms.
8. The adsorption of the tested inhibitor on the metal surface was found to obey the Langmuir adsorption isotherm model.

Author Contributions: Conceptualization, L.M.S. and I.A.A.A.; methodology, A.A.A. and W.N.R.W.I.; software, A.A.A.; validation, I.A.A. and M.S.T.; investigation, M.H.A. and M.H.H.A.-K.; resources, W.N.R.W.I. and M.S.T.; data duration, A.A.A.; writing—original draft preparation, A.A.A.; writing—review and editing, M.M.H. and M.H.H.A.-K.; visualization, M.S.T.; supervision, A.A.A. All authors have read and agreed to the published version of the manuscript.

Funding: This research received no external funding.

Institutional Review Board Statement: Not Applicable.

Informed Consent Statement: Not Applicable.

Data Availability Statement: The data of this study are available from the corresponding author (A.A.A.), upon reasonable request.

Acknowledgments: The authors thank Universiti Kebangsaan Malaysia (Malaysia) and University of Technology (Iraq) for supporting this work.

Conflicts of Interest: The authors declare no conflict of interest.

References

1. Al-Baghdadi, S.B.; Noori, F.T.; Ahmed, W.K.; Al-Amiery, A.A. Thiadiazole as a potential corrosion inhibitor for mild steel in 1 M HCl. *J. Adv. Electrochem.* **2016**, *2*, 67–69.
2. Jawad, Q.S.; Zinad, D.; Dawood Salim, R.; Al-Amiery, A.; Gaaz, T.; Takriff, M.S.; Kadhum, A.A. Synthesis, characterization, and corrosion inhibition potential of novel thiosemicarbazone on mild steel in sulfuric acid environment. *Coatings* **2019**, *9*, 729. [\[CrossRef\]](#)
3. Al-Amiery, A.A.; Ahmed, M.H.O.; Abdullah, T.A.; Gaaz, T.S.; Kadhum, A.A.H. Electrochemical studies of novel corrosion inhibitor for mild steel in 1 M hydrochloric acid. *Results Phys.* **2018**, *9*, 978–981. [\[CrossRef\]](#)
4. Tao, Z.; Zhang, S.; Li, W.; Hou, B. Corrosion inhibition of mild steel in acidic solution by some oxo-triazole derivatives. *Corros. Sci.* **2009**, *51*, 2588–2595. [\[CrossRef\]](#)
5. Ahamad, I.; Quraishi, M.A. Mebendazole: New and efficient corrosion inhibitor for mild steel in acid medium. *Corros. Sci.* **2010**, *52*, 651–656. [\[CrossRef\]](#)
6. Martinez, S. Inhibitory mechanism of mimosa tannin using molecular modeling and substitutional adsorption isotherms. *Mater. Chem. Phys.* **2002**, *77*, 97–102. [\[CrossRef\]](#)
7. Abboud, Y.; Abourriche, A.; Saffaj, T.; Berrada, M.; Charrouf, M.; Bennamara, A.; Hannache, H. A novel azo dye, 8-quinolinol-5-azoantipyrene as corrosion inhibitor for mild steel in acidic media. *Desalination* **2009**, *237*, 175. [\[CrossRef\]](#)
8. Musa, A.Y.; Mohamad, A.B.; Al-Amiery, A.A.; Tien, L.T. Galvanic corrosion of aluminum alloy (Al2024) and copper in 1.0 M hydrochloric acid solution. *Korean J. Chem. Eng.* **2012**, *29*, 818–822. [\[CrossRef\]](#)
9. Kadhim, A.; Al-Amiery, A.A.; Alazawi, R.; Al-Ghezi, M.K.; Abass, R.H. Corrosion inhibitors. A review. *Int. J. Corros. Scale Inhib.* **2021**, *10*, 54–67.
10. Al-Amiery, A.A.; Shaker, L.M. Corrosion inhibition of mild steel using novel pyridine derivative in 1 M hydrochloric acid. *Koroze Ochr. Materiálu.* **2020**, *64*, 59–64. [\[CrossRef\]](#)
11. Alamiery, A.; Mahmoudi, E.; Allami, T. Corrosion inhibition of low-carbon steel in hydrochloric acid environment using a Schiff base derived from pyrrole: Gravimetric and computational studies. *Int. J. Corros. Scale Inhib.* **2021**, *10*, 749–765.
12. Alamiery, A.A. Anticorrosion effect of thiosemicarbazide derivative on mild steel in 1 M hydrochloric acid and 0.5 M sulfuric acid: Gravimetric and theoretical studies. *Mater. Sci. Energy Technol.* **2021**, *4*, 263–273. [\[CrossRef\]](#)
13. Salim, R.D.; Betti, N.; Hanoon, M.; Al-Amiery, A.A. 2-(2, 4-Dimethoxybenzylidene)-N-Phenylhydrazinecarbothioamide as an Efficient Corrosion Inhibitor for Mild Steel in Acidic Environment. *Prog. Color Colorants Coatings.* **2022**, *15*, 45–52.
14. Shaker, L.M.; Al-Adili, A.; Al-Amiery, A.A.; Takriff, M.S. The inhibition of mild steel corrosion in 0.5 M H₂SO₄ solution by N-phenethylhydrazinecarbothioamide (N-PHC). *J. Phys. Conf. Ser.* **2021**, *1795*, 012009. [\[CrossRef\]](#)
15. Alkadir Aziz, I.A.; Annon, I.A.; Abdulkareem, M.H.; Hanoon, M.M.; Alkaabi, M.H.; Shaker, L.M.; Alamiery, A.A.; Wan Isahak, W.N.R.; Takriff, M.S. Insights into Corrosion Inhibition Behavior of a 5-Mercapto-1, 2, 4-triazole Derivative for Mild Steel in Hydrochloric Acid Solution: Experimental and DFT Studies. *Lubricants* **2021**, *9*, 122. [\[CrossRef\]](#)
16. Al-Amiery, A.; Shaker, L.M.; Kadhum, A.A.; Takriff, M.S. Synthesis, characterization and gravimetric studies of novel triazole-based compound. *Int. J. Low-Carbon Technol.* **2020**, *15*, 164–170. [\[CrossRef\]](#)
17. Al-Taweel, S.S.; Al-Janabi, K.W.; Luaibi, H.M.; Al-Amiery, A.A.; Gaaz, T.S. Evaluation and characterization of the symbiotic effect of benzylidene derivative with titanium dioxide nanoparticles on the inhibition of the chemical corrosion of mild steel. *Int. J. Corros. Scale Inhib.* **2019**, *8*, 1149–1169.
18. Salman, T.A.; Al-Amiery, A.A.; Shaker, L.M.; Kadhum, A.A.; Takriff, M.S. A study on the inhibition of mild steel corrosion in hydrochloric acid environment by 4-methyl-2-(pyridin-3-yl) thiazole-5-carbohydrazide. *Int. J. Corros. Scale Inhib.* **2019**, *8*, 1035–1059.

19. Habeeb, H.J.; Luaibi, H.M.; Abdullah, T.A.; Dakhil, R.M.; Kadhum, A.A.; Al-Amiery, A.A. Case study on thermal impact of novel corrosion inhibitor on mild steel. *Case Stud. Therm. Eng.* **2018**, *12*, 64–68. [\[CrossRef\]](#)
20. Salman, T.A.; Jawad, Q.A.; Hussain, M.A.; Al-Amiery, A.A.; Mohamed, L.; Kadhum, A.A.; Takriff, M.S. Novel ecofriendly corrosion inhibition of mild steel in strong acid environment: Adsorption studies and thermal effects. *Int. J. Corros. Scale Inhib.* **2019**, *8*, 1123–1137.
21. ASTM G-31-72; Standard recommended practice for the laboratory immersion corrosion testing of metals. ASTM: Philadelphia, PA, USA, 1990; 401.
22. Migahed, M.A.; El-Rabiei, M.M.; Nady, H.; Elgendy, A.; Zaki, E.G.; Abdou, M.I.; Noamy, E.S. Novel Ionic Liquid Compound Act as Sweet Corrosion Inhibitors for X-65 Carbon Tubing Steel: Experimental and Theoretical Studies. *J. Bio Tribo-Corros.* **2017**, *3*, 31. [\[CrossRef\]](#)
23. Singh, A.; Ebenso, E.E.; Quraishi, M.; Lin, Y. 5,10,15,20-Tetra(4-pyridyl)-21H,23H-porphine as an effective corrosion inhibitor for N80 steel in 3.5% NaCl solution. *Int. J. Electrochem. Soc.* **2014**, *9*, 7495–7505.
24. Farag, A.A.; Noor El-Din, M.R. The adsorption and corrosion inhibition of some nonionic surfactants on API X65 steel surface in hydrochloric acid. *Corro. Sci.* **2012**, *64*, 174–183. [\[CrossRef\]](#)
25. Obot, I.B.; Obi-Egbedi, N.O. Anti-corrosive properties of xanthone on mild steel corrosion in sulphuric acid: Experimental and theoretical investigations. *Curr. Appl. Phys.* **2011**, *11*, 382–392. [\[CrossRef\]](#)
26. Devika, B.G.; Doreswamy, B.H.; Tandon, H.C. Corrosion behaviour of metal complexes of antipyrine based azo dye ligand for soft-cast steel in 1 M hydrochloric acid. *J. King Saud Univ. Sci.* **2020**, *32*, 881–890. [\[CrossRef\]](#)
27. Gerengi, H.; Cakmak, R.; Dagc, B.; Solomon, M.; Tuysuz, A.; Kaya, E. Synthesis and anticorrosion studies of 4-[(2-nitroacetophenonylidene)-amino]-antipyrine on SAE 1012 carbon steel in 15 wt.% HCl solution. *J. Adhes. Sci. Technol.* **2020**, *34*, 1–19. [\[CrossRef\]](#)
28. Hanoon, M.; Zinad, D.S.; Resen, A.M.; Al-Amiery, A.A. Synthesis, characterization and inhibition effect of new antipyrinyl derivatives on mild steel corrosion in acidic solution. *Int. J. Corros. Scale Inhib.* **2020**, *9*, 953–966. [\[CrossRef\]](#)
29. El-Haddad, M.N.; Elattar, K.M. Synthesis, characterization and inhibition effect of new antipyrinyl derivatives on mild steel corrosion in acidic solution. *Int. J. Ind. Chem.* **2015**, *6*, 105–117. [\[CrossRef\]](#)
30. Abd El Rehim, S.; Sibrabim, M.A.M.; Khalid, K.F. The inhibition of 4-(20-amino-50-methylphenylazo) antipyrine on corrosion of mild steel in HCl solution. *Mater. Chem. Phys.* **2001**, *70*, 268–273. [\[CrossRef\]](#)
31. Eldesoky, A.M.; Ghoneim, M.M.; Diab, M.A.; El-Bindary, A.A.; El-Sonbati, A.Z.; Abd El-Kader, M.K. 4-Aminoantipyrine Schiff base derivatives as novel corrosion inhibitors for Q235 steel in hydrochloric acid medium. *J. Mater. Environ. Sci.* **2015**, *6*, 3066–3085.
32. Salman, T.A.; Zinad, D.S.; Jaber, S.H.; Al-Ghezi, M.; Mahal, A.; Takriff, M.S.; Al-Amiery, A.A. Effect of 1, 3, 4-thiadiazole scaffold on the corrosion inhibition of mild steel in acidic medium: An experimental and computational study. *J. Bio Tribo. Corros.* **2019**, *5*, 1–11. [\[CrossRef\]](#)
33. Hanoon, M.M.; Gbashi, Z.A.; Al-Amiery, A.A.; Kadhim, A.; Kadhum, A.A.; Takriff, M.S. Study of Corrosion Behavior of N'-acetyl-4-pyrrol-1-ylbenzohydrazide for Low-Carbon Steel in the Acid Environment: Experimental, Adsorption Mechanism, Surface Investigation, and DFT Studies. *Progress in Color. Colorants Coat.* **2022**, *15*, 133–141.
34. Al-Baghdadi, S.B.; Al-Amiery, A.A.; Kadhum, A.A.; Takriff, M.S. Computational Calculations, Gravimetric, and Surface Morphological Investigations of Corrosion Inhibition Effect of Triazole Derivative on Mild Steel in HCl. *J. Comput. Theor. Nanosci.* **2020**, *17*, 2897–2904. [\[CrossRef\]](#)
35. Hanoon, M.M.; Resen, A.M.; Al-Amiery, A.A.; Kadhum, A.A.; Takriff, M.S. Theoretical and Experimental Studies on the Corrosion Inhibition Potentials of 2-((6-Methyl-2-Ketoquinolin-3-yl) Methylene) Hydrazinecarbothioamide for Mild Steel in 1 M HCl. *Progress in Color. Colorants Coat.* **2022**, *15*, 11–23.
36. Alamiery, A.A. Effect of Temperature on the Corrosion Inhibition of 4-ethyl-1-(4-oxo-4-phenylbutanoyl). *Lett. Appl. NanoBioSci.* **2022**, *11*, 3502–3508.
37. Alamiery, A.A. Corrosion inhibition effect of 2-N-phenylamino-5-(3-phenyl-3-oxo-1-propyl)-1,3,4-oxadiazole on mild steel in 1 M hydrochloric acid medium: Insight from gravimetric and DFT investigations. *Mater. Sci. Energy Technol.* **2021**, *4*, 398–406. [\[CrossRef\]](#)
38. Alamiery, A.A.; Wan Isahak, W.N.; Takriff, M.S. Inhibition of Mild Steel Corrosion by 4-benzyl-1-(4-oxo-4-phenylbutanoyl) thiosemicarbazide: Gravimetric, Adsorption and Theoretical Studies. *Lubricants* **2021**, *9*, 93. [\[CrossRef\]](#)
39. Jamil, D.M.; Al-Okbi, A.K.; Hanon, M.M.; Rida, K.S.; Alkaim, A.F.; Al-Amiery, A.A.; Kadhim, A.; Kadhum, A.A. Carboxythiazole corrosion inhibitor: As an experimentally model and DFT theory. *J. Eng. Appl. Sci.* **2018**, *13*, 3952–3959.
40. Musa, A.Y.; Ahmoda, W.; Al-Amiery, A.A.; Kadhum, A.A.; Mohamad, A.B. Quantum chemical calculation for the inhibitory effect of compounds. *J. Struct. Chem.* **2013**, *54*, 301–308. [\[CrossRef\]](#)
41. Al-Baghdadi, S.; Gaaz, T.S.; Al-Adili, A.; Al-Amiery, A.A.; Takriff, M.S. Experimental studies on corrosion inhibition performance of acetylthiophene thiosemicarbazone for mild steel in HCl complemented with DFT investigation. *Int. J. Low-Carbon Technol.* **2021**, *16*, 181–188. [\[CrossRef\]](#)
42. Al-Amiery, A.; Salman, T.A.; Alazawi, K.F.; Shaker, L.M.; Kadhum, A.A.; Takriff, M.S. Quantum chemical elucidation on corrosion inhibition efficiency of Schiff base: DFT investigations supported by weight loss and SEM techniques. *Int. J. Low-Carbon Technol.* **2020**, *15*, 202–209. [\[CrossRef\]](#)

43. Salman, T.A.; Al-Azawi, K.F.; Mohammed, I.M.; Al-Baghdadi, S.B.; Al-Amiery, A.A.; Gaaz, T.S.; Kadhum, A.A. Experimental studies on inhibition of mild steel corrosion by novel synthesized inhibitor complemented with quantum chemical calculations. *Results Phys.* **2018**, *10*, 291–296. [[CrossRef](#)]
44. Zinad, D.S.; Jawad, Q.A.; Hussain, M.A.; Mahal, A.; Mohamed, L.; Al-Amiery, A.A. Adsorption, temperature and corrosion inhibition studies of a coumarin derivatives corrosion inhibitor for mild steel in acidic medium: Gravimetric and theoretical investigations. *Int. J. Corros. Scale Inhib.* **2020**, *9*, 134–151.
45. Zinad, D.S.; Hanoon, M.; Salim, R.D.; Ibrahim, S.I.; Al-Amiery, A.A.; Takriff, M.S.; Kadhum, A.A. A new synthesized coumarin-derived Schiff base as a corrosion inhibitor of mild steel surface in HCl medium: Gravimetric and DFT studies. *Int. J. Corros. Scale Inhib.* **2020**, *9*, 228–243.
46. Yamin, J.A.; Sheet, E.A.; Al-Amiery, A. Statistical analysis and optimization of the corrosion inhibition efficiency of a locally made corrosion inhibitor under different operating variables using RSM. *Int. J. Corros. Scale Inhib.* **2020**, *9*, 502–518.
47. Umoren, S.A.; Solomon, M.M.; Ali, S.A.; Dafalla, H.D.M. Synthesis, Characterization, and Utilization of a Diallylmethylamine-Based Cyclopolymer for Corrosion Mitigation in Simulated Acidizing Environment. *Mater. Sci. Eng. C* **2019**, *100*, 897–914. [[CrossRef](#)]
48. El-Lateef, H.M.A. Corrosion inhibition characteristics of a novel salicylidene isatin hydrazine sodium sulfonate on carbon steel in HCl and a synergistic nickel ions additive: A combined experimental and theoretical perspective. *Appl. Surf. Sci.* **2020**, *501*, 144237. [[CrossRef](#)]
49. Onyeachu, I.B.; Obot, I.B.; Sorour, A.A.; Abdul-Rashid, M.I. Green corrosion inhibitor for oilfield application I: Electrochemical assessment of 2-(2-pyridyl) benzimidazole for API X60 steel under sweet environment in NACE brine ID196. *Corros. Sci.* **2019**, *150*, 183–193. [[CrossRef](#)]
50. Umoren, S.A.; Solomon, M. Protective polymeric films for industrial substrates: A critical review on past and recent applications with conducting polymers and polymer composites/nanocomposites. *Prog. Mater. Sci.* **2019**, *104*, 380–450. [[CrossRef](#)]
51. Solmaz, R.; Kardaş, G.; Çulha, M.; Yazıcı, B.; Erbil, M. Investigation of adsorption and inhibitive effect of 2-mercaptothiazoline on corrosion of mild steel in hydrochloric acid media. *Electrochim. Acta* **2008**, *53*, 5941–5952. [[CrossRef](#)]
52. Solomon, M.M.; Umoren, S.A.; Quraishi, M.A.; Tripathi, D.; Abai, E.J. Effect of Akyl Chain Length, Flow, and Temperature on the Corrosion Inhibition of Carbon Steel in a Simulated Acidizing Environment by an Imidazoline-Based Inhibitor. *J. Pet. Sci. Eng.* **2020**, *187*, 106801. [[CrossRef](#)]